© 2016. Published by The Company of Biologists Ltd | Development (2016) 143, 3168-3181 doi:10.1242/dev.134254

RESEARCH ARTICLE

Eye development and photoreceptor differentiation in the cephalopod *Doryteuthis pealeii*

Kristen M. Koenig[1,‡,§], Peter Sun[1], Eli Meyer[2] and Jeffrey M. Gross[1,*,§]

ABSTRACT

Photoreception is a ubiquitous sensory ability found across the Metazoa, and photoreceptive organs are intricate and diverse in their structure. Although the morphology of the compound eye in *Drosophila* and the single-chambered eye in vertebrates have elaborated independently, the amount of conservation within the 'eye' gene regulatory network remains controversial, with few taxa studied. To better understand the evolution of photoreceptive organs, we established the cephalopod *Doryteuthis pealeii* as a lophotrochozoan model for eye development. Utilizing histological, transcriptomic and molecular assays, we characterize eye formation in *Doryteuthis pealeii*. Through lineage tracing and gene expression analyses, we demonstrate that cells expressing *Pax* and *Six* genes incorporate into the lens, cornea and iris, and the eye placode is the sole source of retinal tissue. Functional assays demonstrate that Notch signaling is required for photoreceptor cell differentiation and retinal organization. This comparative approach places the canon of eye research in traditional models into perspective, highlighting complexity as a result of both conserved and convergent mechanisms.

KEY WORDS: Squid, Eye evolution, Lophotrochozoa, Cephalopod

INTRODUCTION

In *On the Origin of Species*, Darwin marveled at the capacity of natural selection to produce the eye as an 'organ of extreme perfection and complication' (Darwin, 1859). It is the exacting intricacy of photoreceptive organs that provides an elegant system to study the emergence of complexity. The capacity for photoreception is a sensory tool that evolved early in the Metazoa (Schnitzler et al., 2012). The extent of this capacity ranges from single photoreceptor cells, pigmented eyespots and cups, to complicated organs that focus, reflect and absorb light to resolve images (Land and Fernald, 1992). In the Bilateria, high-resolution vision is known to have evolved in only a few animal groups, including vertebrates, arthropods and cephalopods (Nilsson, 2013). The arthropod eye is a compound eye composed of many individual ommatidial units containing multiple photoreceptor cells and a lens. Both the vertebrate and the cephalopod eye are single-chambered, with a single lens at the anterior of the eye and a cup-shaped retina in the posterior. Despite the use of a similar optical strategy, these two eye structures have evolved independently (Fernald, 2006).

The incredible diversity in eye shape and photoreceptor cell structure in animals led Salvini-Plawen and Mayr to conclude that the eye had evolved independently ~40-65 times (von Salvini-Palwen and Mayr, 1977). With the expansion of molecular tools, however, extensive genetic analyses in *Drosophila* and vertebrates demonstrated that many orthologous genes and signaling pathways are necessary for eye formation. The Pax-Six-Eya-Dach network [also known as the retina determination network (RDN)] occupies the nexus of this genetic homology. *Eyeless*, *twin of eyeless* (Pax6 ortholog), *sine oculis* (Six1 and Six2 ortholog), *eya* and *dac* (Dach ortholog) are all necessary for eye development in *Drosophila* (reviewed by Kumar, 2010). They each can induce ectopic eye formation when mis-expressed in the antennal imaginal disc. In vertebrates, Pax6, Six3 and Six6 (*optix* homologs), Eya1, Eya2, Eya3 and Dach1 are each known to play a role in eye development. Among these, Pax6, Six3 and Eya3 can also induce ectopic retina and lens formation when mis-expressed in vertebrates (reviewed by Tomarev, 1997; Arendt, 2003; Nilsson, 2004; Kumar, 2010; Wagner, 2014).

The Notch signaling pathway also plays essential roles during retina and lens formation in vertebrates and *Drosophila*. Notch activity regulates cell cycle progression within the retina and lens, and regulation of Notch activity is necessary for maintenance of progenitor cell populations (Livesey and Cepko, 2001; Charlton-Perkins et al., 2011a). In vertebrates, retinal progenitor cells deficient in Notch signaling prematurely exit the cell cycle, which results in a smaller retina and a higher proportion of early-born cell types (Tomita et al., 1996; Dorsky et al., 1997). In *Drosophila*, loss of Notch signaling reduces imaginal disc proliferation and can lead to a smaller eye (Cagan and Ready, 1989; Go et al., 1998). Notch also regulates photoreceptor cell fate and ommatidial polarity (Blair, 1999).

This extensive amount of similarity has led many to conclude that all photoreceptive organs have a shared ancestry (Halder et al., 1995; Gehring, 1996, 2005; Gehring and Ikeo, 1999; Tomarev, 1997). Others suggest that, despite the inclusion of the same gene families, the regulatory networks underlying eye development in vertebrates and *Drosophila* are fundamentally different in their connectivity and are therefore likely to have evolved independently (Wagner, 2014). To address the homology of photoreceptive organs in the Bilateria and to better recognize the novelty found in each of these systems, it is necessary to understand the functional relationships between these genes in taxa beyond *Drosophila* and vertebrate models. A comparative approach that includes lophotrochozoan species sheds light on shared molecular mechanisms that operate during organ formation and informs an understanding of the conservation of regulatory modules throughout the Bilateria.

[1]Department of Molecular Biosciences, Institute for Cellular and Molecular Biology, University of Texas at Austin, Austin, TX 78712, USA. [2]Department of Zoology, Oregon State University, Cordley Hall 3029, Corvallis, OR 97331, USA.
[‡]Present address: FAS Center for Systems Biology, Harvard University, Northwest Labs 365.10, 52 Oxford Street, Cambridge, MA 02138, USA. *Present address: Eye and Ear Institute, Charles and Louella Snyder Laboratory for Retinal Regeneration, Department of Ophthalmology, Louis J. Fox Center for Vision Restoration, University of Pittsburgh School of Medicine, Pittsburgh, PA 15213, USA.

[§]Authors for correspondence (grossjm@pitt.edu; kmkoenig@gmail.com)

J.M.G., 0000-0002-9422-6312

Received 22 December 2015; Accepted 25 July 2016

Development (2016) 143, 3168-3181 doi:10.1242/dev.134254

The squid *Doryteuthis pealeii* is a tractable lophotrochozoan model for studying complex eye development and understanding these networks. Cephalopods have the largest and most complex invertebrate nervous system and *Doryteuthis pealeii* has long been the subject of neurobiological and neurophysiological research (e.g. Hodgkin and Katz, 1949; Hodgkin and Huxley, 1952a,b; Hodgkin et al., 1952; Vale et al., 1985a,b; Brady et al., 1982; Allen et al., 1982). Moreover, adult neuroanatomy of multiple cephalopod species has been well described (Young, 1962a,b, 1971; Nixon and Young, 2003; Wild et al., 2015). Despite these elegant studies, gene expression is only now being explored during development, and detailed molecular and genomic analyses of cephalopod organogenesis are in their infancy (Tomarev et al., 1997; Hartmann et al., 2003; Lee et al., 2003; Baratte et al., 2007; Farfán et al., 2009; Navet et al., 2009; Buresi et al., 2012, 2013, 2016; Ogura et al., 2013; Focareta et al., 2014; Peyer et al., 2014; Wollesen et al., 2014; Yoshida et al., 2014; Shigeno et al., 2015; Wollesen et al., 2015). The cephalopod eye is a single-chambered eye generated from an internalization of the optic placode (Gilbert et al., 1990). The single lens is produced by populations of specialized lentigenic cells and is located at the anterior of the eye (West et al., 1994, 1995). The retina, composed of rhabdomeric photoreceptor cells and a support cell layer, is located at the posterior of the eye (Zonana, 1961; Wild et al., 2015). Photoreceptor outer segments are arrayed anteriorly and thus, are the first region of the retina to be exposed to light. This differs from the vertebrate eye where light must traverse the retina prior to interacting with photoreceptors. In the cephalopod, photoreceptor nuclei are located at the posterior of the retina, and photoreceptor axons form a plexiform layer behind this nuclear layer, exiting the eye and synapsing directly on the optic lobe (Young, 1971; Wild et al., 2015). General descriptions of eye development in various cephalopod species have been documented, but an in-depth molecular and cellular understanding of major morphogenetic and cell differentiation events is lacking (Arnold, 1965, 1966, 1967; Arnold and Williams-Arnold, 1976; Gilbert et al., 1990; Marthy, 1973; Yamamoto, 1985; Yamamoto et al., 1985; Naef, 1928). Recently, the cephalopod genomic infrastructure was greatly improved by publication of the *Octopus bimaculoides* genome and a few transcriptomic databases (Albertin et al., 2015; Alon et al., 2015; Yoshida, 2011; Wollesen et al., 2014; Bassaglia et al., 2012). Despite these improvements, however, few sequencing efforts have informed our understanding of embryonic development or organogenesis.

Here, we utilize a variety of histological, transcriptomic and molecular assays to identify developmental landmarks of eye formation in *D. pealeii*. This lophotrochozoan resource demonstrates the power of comparative developmental biology and begins to unravel mechanisms underlying the emergence of eye complexity. For example, despite the independent origin of the cephalopod lens, many orthologous transcription factors involved in lens development in *Drosophila* and vertebrates are expressed in lens progenitor cells of the cephalopod, underscoring that transcriptional cascades are often convergent in their functions across the Bilateria. We also demonstrate that Notch maintains a progenitor pool in the cephalopod retina, as it does in vertebrates and *Drosophila.* This is the first evidence that Notch may be acting in a conserved manner in the context of a pseudostratified neuroepithelium in the Lophotrochozoa. Ultimately, this highlights a possible common cellular mechanism to generate neuronal diversity in neuroepithelia within the Bilateria.

RESULTS

Morphogenesis, growth and patterning of the cephalopod eye

To provide a foundation to build a molecular and cellular understanding of eye development in *D. pealeii*, it was necessary to generate a detailed histological description of eye formation. All staging nomenclature follows Arnold (1965). Eye development commences at stage 16 with the formation of bilateral placodes shortly before epiboly is complete (Fig. 1). Beginning at stage 18, these placodes are internalized when a lip of cells forms around the periphery of the placode and progressively closes, fusing centrally at stage 21 to form the optic vesicles (Fig. 2; Fig. S1) (Gilbert et al., 1990; Marthy, 1973). Once the vesicle is closed, the eye continues to grow and the retina begins to curve. At stage 22, cells at the anterior of the vesicle begin to differentiate into the primary and secondary lentigenic cells, which project cellular processes that form the segmented extracellular lens (Fig. 3A and Fig. 4) (Arnold, 1967; West et al., 1995). These cells have a distinct nuclear architecture and are enriched in filamentous actin (Fig. 2, Fig. 3B and Fig. 4). At hatching (post stage 29), the retina is primarily composed of two cell types: photoreceptors and glial-like support cells (Young, 1971).

Between stage 18 and stage 26, the neuroepithelium appears as a single layer with no obvious morphological distinction between photoreceptors and glial-like support cells. At stage 27, photoreceptor nuclei in the posterior retina begin to segregate to the basal side of the epithelium. This segregation initiates asymmetrically behind the basal membrane, suggesting a progressive wave of differentiation moving from the posterior of the animal to anterior (Fig. 2, Fig. 3C and Fig. 4) (Yamamoto, 1985; Yamamoto et al., 1985). Photoreceptors penetrate the basal membrane, extending through the support cell layer, forming outer segments on the apical side of the retina. Outer segments are prominently labeled with Phalloidin. Photoreceptors synapse directly on the optic lobe (Young, 1971; Wild et al., 2015). At hatching, the eye is functional (Gilbert et al., 1990).

The apical side of the retinal neuroepithelium faces anteriorly and progenitor cells consistently undergo mitosis on the apical side of the retina (Fig. 2, Fig. 3C and Fig. 4) similar to neuroepithelia in other organisms (Baye and Link, 2008). To determine the pattern of progenitor cell cycle exit in the retina, we performed a series of BrdU incorporation assays. All cells of stage 19-25 retinae incorporate BrdU (Fig. 5A-D). At stage 25, two populations of $BrdU^+$ cells are detected (Fig. 5D). Cells on the basal side of the retina incorporate BrdU, as expected if they are in S-phase during the exposure window. Mitotic cells on the apical side of the retina are also $BrdU^+$, suggesting that they passed through S-phase earlier in the exposure window. At stage 27, once photoreceptor nuclei have migrated behind the basal membrane, they no longer incorporate BrdU, suggesting that they are not proliferative (Fig. 5E-G). Interestingly, the support cell layer continues to incorporate BrdU until at least 2 days post-hatching (Fig. 5G) and nuclei are observed crossing from one side of the basal membrane to the other (Fig. 4). Without *in vivo* tracking, it is unknown whether these nuclei move from the support cell layer to the photoreceptor cell layer across the basal membrane, or vice versa. However, given the lack of BrdU incorporation by nuclei on the photoreceptor side of the basal membrane and the rapid growth of the eye after hatching, newly generated photoreceptors may arise from support cell layer-derived cells.

Apoptosis contributes significantly to eye formation in vertebrates and *Drosophila* and we were interested to determine

Development (2016) 143, 3168-3181 doi:10.1242/dev.134254

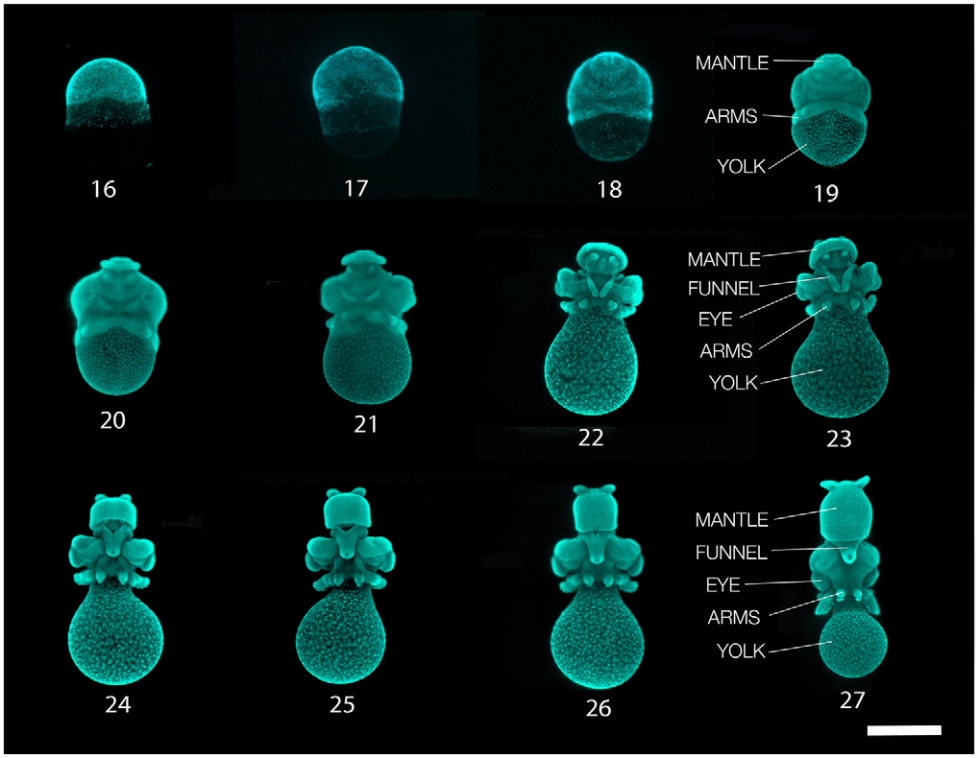

Fig. 1. Embryonic stages and transcriptome of *Doryteuthis pealeii*. Sytox Green-stained embryos at stages 16-27 (Arnold, 1965). Posterior view. Each stage is sequenced to generate a whole-embryo transcriptome. Scale bar: 1 mm.

whether cell death played a role in eye morphogenesis in squid (Baker, 2001; Vecino et al., 2004). Surveys for apoptosis, using TUNEL as a marker, did not reveal an appreciable number of apoptotic cells during eye development (Fig. 6).

Lineage tracing of the eye placode and surrounding tissues identifies retina, lens and brain progenitors

Previous studies suggested fates for specific populations of cells in and around the eye placode of various cephalopod species, but no detailed lineage tracing study exists (Yamamoto et al., 2003; Marthy, 1987). These data are crucial to correlate gene expression data with distinct fates in the eye and compare neurogenesis between cephalopods and other systems. With this in mind, we generated a fate map of the eye placode and surrounding tissue. Populations of cells were labeled with DiI at stage 18 (Fig. 7A,B), immediately documented (Fig. 7C) and embryos were grown to hatching stage, at which point they were fixed and photographed (Fig. 7D). A subset were sectioned and imaged by confocal microscopy (Fig. 7E). A total of 246 embryos were labeled and scored as whole mounts, and 74 were sectioned and imaged. Representative examples of whole-mount and section data are presented in Fig. 8. Lineage tracing confirmed some previously identified cell contributions to eye and

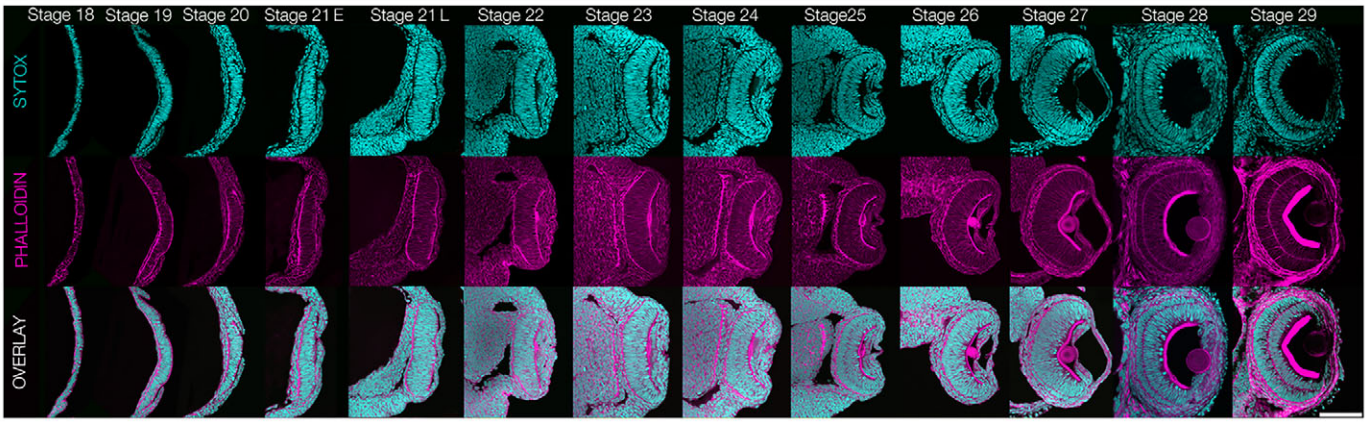

Fig. 2. Staging series of eye development in *D. pealeii*. Embryonic stages 18-29 in cross-section. Anterior of the animal is up in all images. Stage 18: placode has formed and the lateral edge of the lip is present. Stage 19: medial and lateral lip are present and placode neuroepithelium formed. Stage 20: lips of the placode are apposed and apical divisions detected in the retina. Stage 21 early (E): placode lips fuse forming the optic vesicle. Stage 21 late (L): pseudostratified epithelium of the retina grows along the apical-basal axis. Stage 22: retina begins to curve and lens is apparent. Stage 23: plexiform layer in the optic lobe is apparent. Stage 24: lentigenic cell morphology becomes obvious. Stage 25: the lens has grown and is teardrop shaped, outer segment formation of photoreceptor cells beginning. Stage 26: F-actin accumulation in the lentigenic cells. Stage 27: basal membrane in the retina begins to form and photoreceptor nuclei segregate at the posterior retina. Stage 28: the basal membrane and a layer of photoreceptor cell nuclei span the retina. Vasculature is present. Stage 29: photoreceptor cell layer has grown significantly and outer segments are substantial. Scale bar: 50 µm. DNA is stained with Sytox Green and F-actin with Phalloidin.

Development (2016) 143, 3168-3181 doi:10.1242/dev.134254

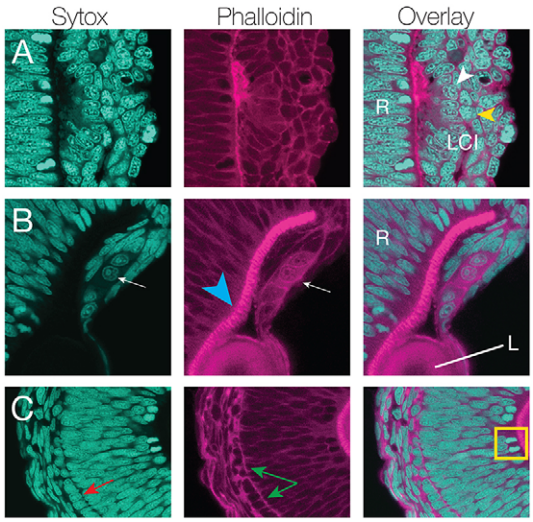

Fig. 3. High magnification staging series of *D. pealeii* embryos. (A) Stage 22. Retina to the left (R), lens and iris to the right (LCI). White arrowhead indicates primary lentigenic cells; yellow arrowhead, secondary lentigenic cells. (B) Stage 27. Retina (R) and lens (L). Blue arrowhead indicates F-actin enrichment in outer segments; white arrow indicates lentigenic cells. (C) Stage 27 retina. Red arrow indicates photoreceptor nuclei segregating at the posterior of the retina; green arrows indicate the basal membrane. Yellow box surrounds cells that have just divided on the apical side of the retina.

brain lobe primordia, but also identified new progenitor populations (Yamamoto et al., 2003). Cells labeled within the placode were found primarily in the retina and placode cells were the only cells that contributed to the retina (Fig. 8A,G). Punctate label from placode cells was also detected in the optic lobe, primarily in the plexiform layer. While this can probably be attributed to transfer along photoreceptor axons, the possibility that placode cells incorporate into the optic lobe cannot be discounted. Interestingly, cells at the lip of the placode incorporated only into lens and iris tissue (Fig. 8B,H). These data suggest that the cephalopod eye is composed entirely of cells derived from these two neighboring tissues: the placode and placode lip.

Optic lobe primordia cells are located dorsal and lateral to the placode. The cells labeled in the more medial portion of this optic lobe-fated region also incorporate into the anterior chamber organ (Fig. 8C,D,I,J). Cells medial and medial-ventral to the placode incorporated into the supraesophageal mass (cerebral ganglia), buccal mass and buccal ganglia (Fig. 8E,K). Cells ventrolateral to the placode incorporated into the subesophageal mass (pedal ganglia) (Fig. 8F,L). See below for placode-stage lineages mapped onto three-dimensional rendering of neuroganglia in a hatching stage embryo generated through microCT scanning (Kerbl et al., 2013).

Development of embryonic transcriptomic resources for *D. pealeii*

Although next-generation sequencing has advanced non-model systems, large-scale genomic infrastructure and in-depth transcriptomic databases in the Lophotrochozoa, remain lacking. With this in mind, and our goal of identifying genes and regulatory networks that facilitate eye development in *Doryteuthis pealeii*, it was necessary to establish a transcriptomic database for embryogenesis and eye morphogenesis. We could then evaluate candidate eye development genes *en masse* and correlate temporal expression to focus our expression and functional analysis. To achieve this, a pooled embryonic transcriptome of 12 stages of

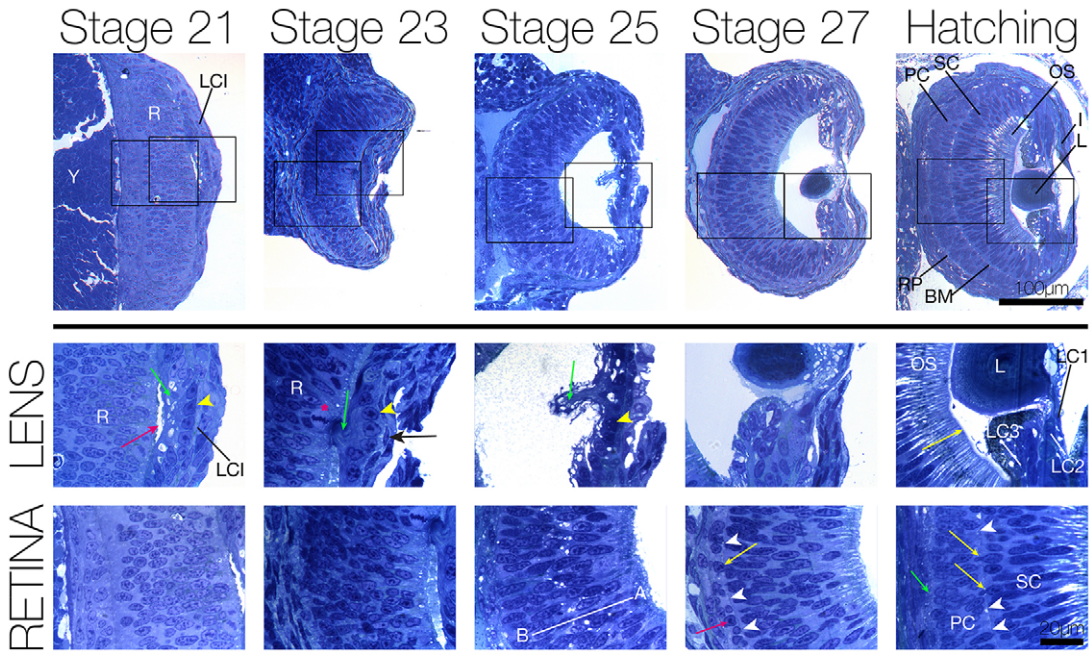

Fig. 4. Histological staging series of *D. pealeii* embryos. Boxed regions are high-magnification images of developing lens and retina shown below each stage. Stage 21 lens: yellow arrowhead indicates lentigenic cells; green arrow, lentigenic cell processes; pink arrow, formation of vitreous cavity. Stage 23 lens: pink asterisk, mitotic cell on apical side of retina; black arrow, primary lentigenic cells (LC1); yellow arrowhead, secondary lentigenic cells (LC2); green arrow, lentigenic cell processes. Stage 25 lens: yellow arrowhead, secondary lentigenic cells; green arrow, lentigenic cell processes and lens. Stage 25 retina (R): apical (A) and basal (B) axis is labeled. Stage 27 retina: pink arrow, newly born photoreceptor nuclei (PC); white arrowheads, basal membrane (BM); yellow arrow, nucleus crossing the basal membrane. Hatching lens: yellow arrow, limiting membrane. Hatching retina: white arrowheads, basal membrane; yellow arrows: nuclei crossing the basal membrane; green arrow, retina plexiform layer. I, iris; LC3, tertiary lentigenic cells; LCI, lens, cornea and iris; OS, outer segment (also known as distal segment); SC, support cell layer; Y, yolk.

Development (2016) 143, 3168-3181 doi:10.1242/dev.134254

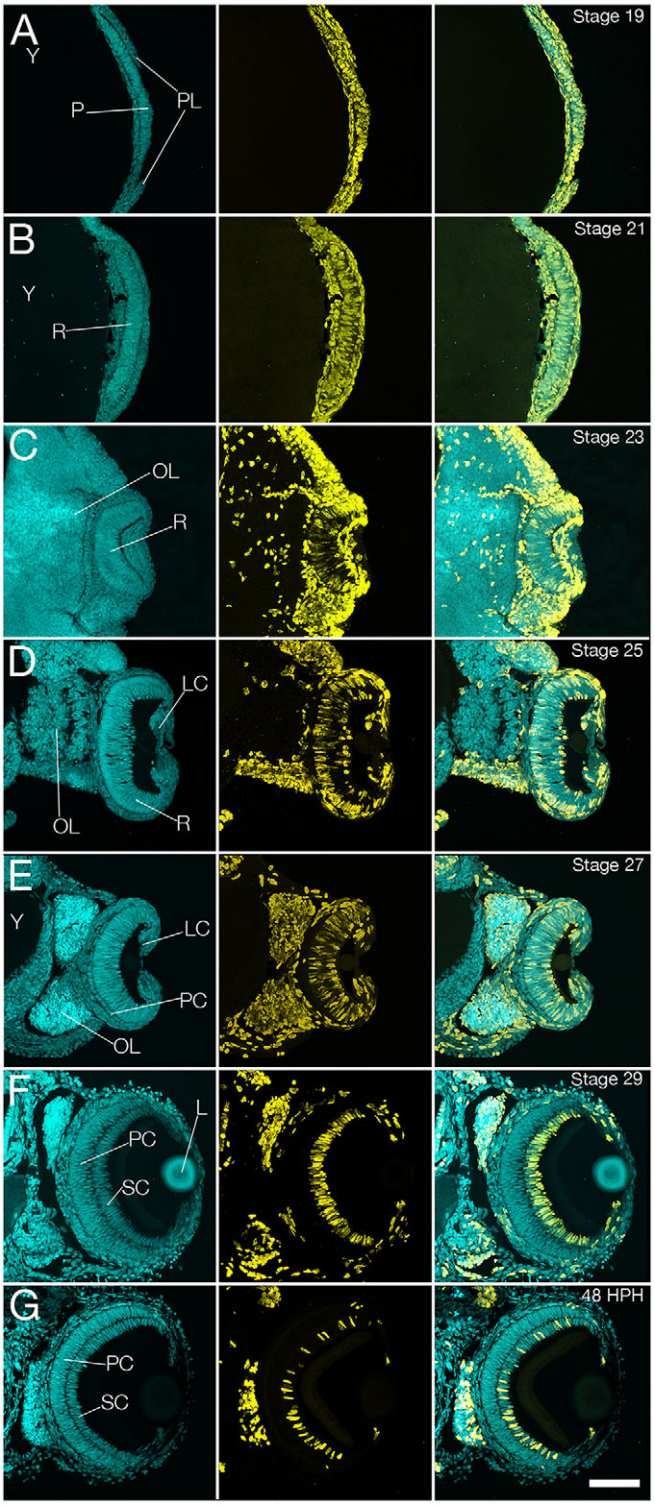

Fig. 5. BrdU incorporation assays reveal spatial patterns of cell proliferation during retina development. Sytox Green stains DNA and BrdU staining is yellow. Embryos were pulsed with BrdU for 3 h and immediately fixed. (A-C) BrdU incorporation is detected broadly throughout the retina at stages 19, 21, and 23. (D) BrdU incorporation begins to segregate to cells on the apical and basal sides of the epithelium. (E) Photoreceptor cell nuclei located behind the basal membrane no longer incorporate BrdU. (F) Support cells and lens and iris continue to incorporate BrdU. (G) Two days post-hatching, support cell layer and lentigenic cells continue to incorporate BrdU. Scale bar: 50 µm. L, lens; LC, lentigenic cells; OL, optic lobe; PC, photoreceptor cell nuclei; P, placode; PL, placode lip; R, retina; SC, support cell nuclei; Y, yolk.

development (stages 16-27) was sequenced, assembled *de novo* and annotated. In addition, RNA-seq data from dissected placode tissue and eye and optic lobe tissues were generated from five developmental stages (19, 21, 23, 25, 27). Each developmental stage was sequenced in biological triplicate (see Materials and Methods for details).

The eye is unusual because it contains cells with conserved functions, such as opsin-expressing photoreceptor cells, in the context of a complex and independently evolved organ. As a result, we expected to identify both conserved molecular markers as well as genes previously unassociated with photoreceptive organs. We were able to assess the presence of candidate eye genes as a first step to determine homoplasy or conserved functionality in cell and tissue identity networks. Moreover, the time-course RNA-seq data provided a quantitative assessment of gene expression over time.

During analysis, we generated a heatmap of transcription factors with dynamic expression (Fig. 9). Looking closely at two representative clusters, genes involved in eye development in other systems are well represented. For example, Lim factors, Pou family members and *Barh* are known to be essential in many neurodevelopmental contexts and are important in vertebrate and *Drosophila* eye development (Hobert and Westphal, 2000; Rosenfeld, 1991; Reig et al., 2007). Pou expression has also been shown in late stage development of the eye in the squid *Idiosepius notoides* (Wollesen et al., 2014). *cut* is necessary for cone cell differentiation and lens formation in *Drosophila* and neural retina-specific leucine zipper protein (*Nrl*) functions during vertebrate retinal cell differentiation (Mears et al., 2001; Nepveu, 2001). Interestingly, the transcription factor *Ovo*, enriched early in our dataset, functions during eye regeneration in the planarian *Schmidtea mediterranea* (Lapan and Reddien, 2012). Importantly, the expression of these genes does not differentiate between conserved and convergent functions within eye development and despite the occurrence of many transcription factors necessary for eye development in other systems, we also identified a number that are as yet unexplored in the visual system (i.e. Abdominal-B/Post2, Knot, Hhex, Hepatic leukemia factor). These genes may have evolved a novel function in cephalopods, or we may be witnessing a cryptic function previously unidentified in other systems.

Expression of genes involved in vertebrate and *Drosophila* eye development

This developmentally focused transcriptome provides broad coverage of candidate transcription factors, transcriptional cascades and signaling pathways known to be involved in *Drosophila* and vertebrate eye development. As discussed above, the Pax6 transcriptional cascade (RDN) and Notch signaling pathway both play essential roles during eye formation in other taxa and these genes displayed interesting changes in expression over time (Fig. 10). *Pax6*, *Six* genes, *Prospero* and *Eyes absent* all were more highly represented at early stages in our dataset. Expression of Notch pathway genes was also interesting. *Notch* was expressed throughout eye development and was enriched at later stages. One Delta family member and all Hes family members, except for Isogroup00902, mirrored *Notch* expression.

We were interested in these candidate eye genes and how Notch might be functioning during neurogenesis. To begin to address this, we cloned *Pax6*, *Six3*, *Six2*, *Pax2*, *Eyes absent*, *Notch*, *Hes* (Isogroup00502) and *Prospero*. Sequence alignment and maximum-likelihood phylogenetic analyses confirmed orthology (Fig. S3). *In situ* hybridizations identified spatial patterns of expression (Fig. 11; Fig. S2), which were then correlated with the

Development (2016) 143, 3168-3181 doi:10.1242/dev.134254

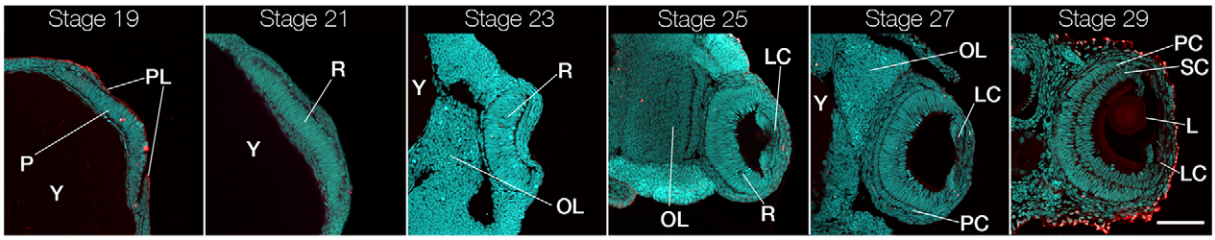

Fig. 6. TUNEL assays on the eye in *D. pealeii* embryos at stages 19, 21, 23, 25, 27 and 29. Sytox Green-labeled DNA (cyan) and TUNEL (red). Few TUNEL^{+} cells are detected. Red cells at stage 29 are in the dermal tissue and are likely to be background from the iridophores. L, lens; LC, lentigenic cells; OL, optic lobe; P, placode; PC, photoreceptor cell nuclear layer; PL, placode lip; R, retina; SC, support cell nuclear layer; Y, yolk.

stage 18 fate map, enabling us to predict the terminal fates of cells expressing specific genes (Figs 11 and 12).

At stage 18, *Notch*, *Hes*, *Prospero* and *Eyes absent* were each expressed in cells of the placode, which give rise to the retina. *Notch* expression was detected asymmetrically on the ventral side of the placode and also in the surrounding extraocular tissue. *Hes* expression was variable; at stage 18, *Hes* was detected in only a portion of the placode, while at stage 19, Hes was expressed throughout the entire placode (Fig. 11). *Hes* expression in the retina continued through stage 27 (Fig. S2F; Figs 11 and 13). *Prospero* was expressed in a punctate pattern at the ventral edge of the placode. *Eyes absent* was expressed throughout the placode, but asymmetrically, with more signal detected on the ventral edge. *Eyes absent* was also detected in tissue surrounding the placode. *Pax6*, *Pax2* and *Six3* are all expressed in the lip cells surrounding the placode. These cells give rise to the lens and iris. *Pax6* expression was detected broadly, dorsal and lateral to the placode, in the region of cells contributing to the optic lobe. *Six3* was expressed only medial to the placode, in the region contributing to the cerebral ganglia. *Pax2* was expressed in cells of the lip as well as in distinct stripes dorsal to the placode, in the optic lobe progenitor region. *Pax2* was also prominently expressed in the developing arms. Finally, *Six2* was expressed in the tissue just ventral and lateral to the placode. Interestingly, while Pax and Six genes were expressed in the retina at later stages of development (Fig. S2A,B,D,E), expression was not detected in the placode at stage 18. However, we cannot rule out the possibility that they are expressed at a level below the threshold for detection. Fig. 12 summarizes placode stage gene expression patterns associated with cell fates in the hatching stage embryo.

Loss of Notch signaling leads to retina disorganization and premature cell cycle exit

Our lineage-tracing data confirmed that placode tissue incorporated into the retina, and gene expression studies indicated that Notch pathway members were expressed in placode cells. Thus, we were interested in whether Notch signaling functioned during retina formation in squid, and more specifically, whether the Notch pathway regulates progenitor maintenance as it does in vertebrates and *Drosophila*. *In vivo* transfection methods or genome editing techniques have not been developed in any cephalopod species, making targeted loss-of-function studies difficult. To circumvent this, we treated embryos with the well-characterized Notch inhibitor DAPT to determine how Notch signaling impacts retina formation (Geling et al., 2002). Embryos were treated for 24 h and allowed to recover until vehicle controls reached stage 27. To assess the efficacy of DAPT, *in situ* hybridization for *Hes* was performed, providing a useful readout of active Notch signaling. Control embryos maintained robust *Hes* expression, while treated embryos lacked *Hes* expression completely, confirming an effective knockdown of Notch pathway activity by DAPT (Fig. 13A).

DAPT-treated embryos were microphthalmic and lacked retina pigmentation. In sectioned samples, the retina was completely disorganized: the basal membrane was absent, morphologically distinct photoreceptor cells were not detectable and there was no defined photoreceptor layer (Fig. 13B). Lentigenic cells and lens formation appeared normal, suggesting that the effects of blocking Notch pathway activity are specific to the retina. Three hours after DAPT treatment, apoptotic cell numbers did not differ from the wild type, indicating that apoptosis is not an immediate response to DAPT treatment (Fig. S4). Apoptotic cells were observed in the retina after an extended recovery period, however, which is similar to the loss of Notch signaling in the vertebrate retina (Tomita et al., 1996).

These data suggest that Notch signaling is required for photoreceptor cell differentiation in the squid retina. To further test this hypothesis, we performed an *in situ* hybridization for the photoreceptor cell marker, *Rhodopsin*. In control embryos, *Rhodopsin* is robustly expressed in the retina. However, in DAPT-

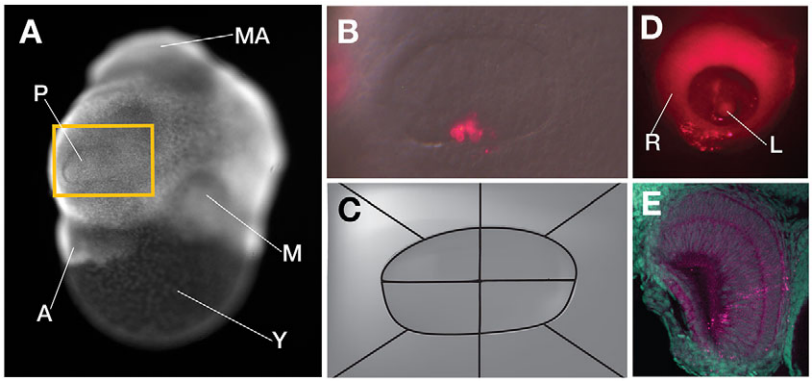

Fig. 7. DiI lineage tracing experimental design. (A) Stage 18 eye placode (gold box). (B) DiI labeling. (C) Labeled cells were assigned on a map of the placode region. At least 20 embryos labeled in each of the 10 regions. (D) Embryos were grown until hatching stage, fixed and photographed in whole mount. Lateral view of the eye shown with labeled cells in the retina. (E) Embryos cryosectioned into serial 12 µm sections, counterstained with Sytox Green, and imaged using confocal microscopy. In this example, DiI label is detected in the support cell layer and the photoreceptor layer of the retina. A, arm; M, mouth; MA, mantle; P, placode; Y, yolk.

Development (2016) 143, 3168-3181 doi:10.1242/dev.134254

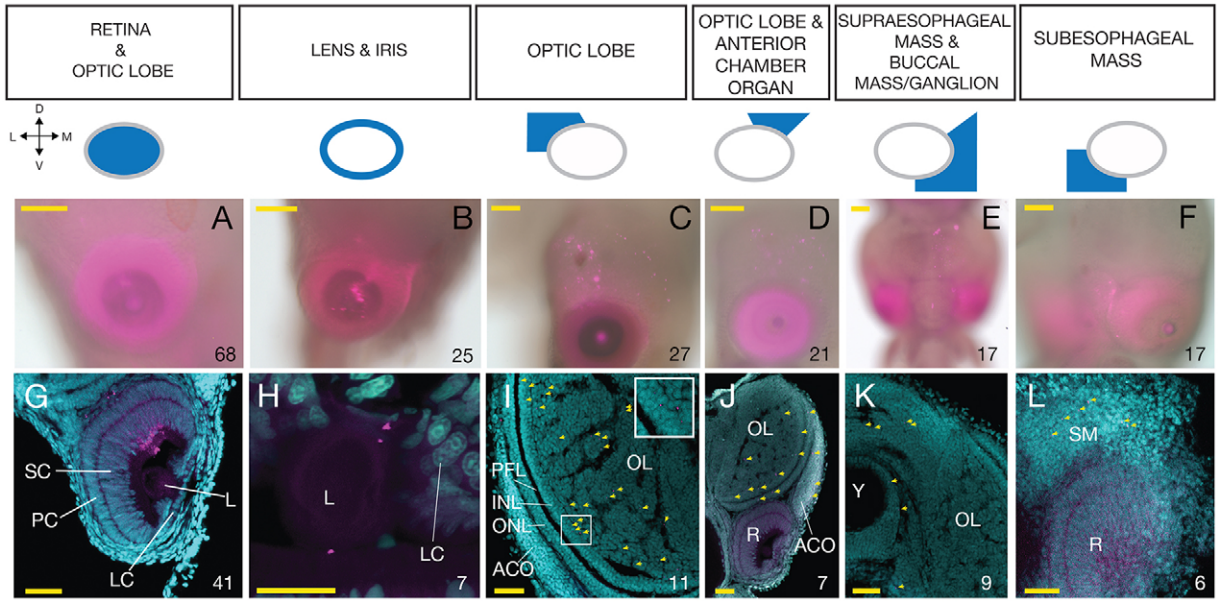

Fig. 8. Dil lineage tracing results. Representative examples of progenitor domains identified in the placode stage lineage tracing experiment. Cartoons at the top of the figure show the stage 18 location of cells. Below each cartoon is whole-mount image (A-F) and sectioned examples (G-L). DNA is labeled with Sytox Green. Yellow arrows highlight Dil puncta. Inset in I shows high-magnification image of puncta. Number of replicates obtained is indicated on each image. (A,G) Cells within the placode are the only cells that incorporate into the retina. (B,H) The placode lip generates the lens and iris. (C-F,I-L) Regions surrounding the placode and placode lip incorporate into specific brain regions. Scale bar: 100 µm in A-F, 50 µm in G,I-L, 25 µm in H. ACO, anterior chamber organ; INL, inner nuclear layer; L, lens; LC, lentigenic cells; OL, optic lobe; ONL, outer nuclear layer; PC, photoreceptor cell nuclear layer; PFL, plexiform layer; R, retina; SC, support cell nuclear layer; SM, subesophageal mass; Y, yolk.

treated animals, *Rhodopsin* expression is lost (Fig. 13C). Retinal cells in DAPT-treated embryos could either remain in a progenitor-like, undifferentiated state or they could prematurely exit the cell cycle and differentiate into a cell type other than a rhodopsin-expressing photoreceptor. To distinguish between these possibilities, we performed BrdU incorporation assays. While control embryos incorporated BrdU normally, DAPT-treated embryos contained no $BrdU^{+}$ retinal cells (Fig. 13D). These data support the model that Notch activity is required to maintain neural progenitors. To determine if the prematurely differentiating retinal cells retained a neural fate, we performed *in situ* hybridization for the neural marker *Neural filament 70* (*NF70*) (Szaro et al., 1991). Retinal cells in DAPT-treated embryos were positive for *NF70* suggesting that, although they are not photoreceptors, they did differentiate into a neural cell type (Fig. 13E).

DISCUSSION

Doryteuthis pealeii as a model for the evolution of the visual system and neural complexity

The past 15 years have seen consistent growth in the molecular accessibility of lophotrochozoan systems (Henry et al., 2010; Gentile et al., 2011; Ferrier, 2012; Zantke et al., 2014; Simakov

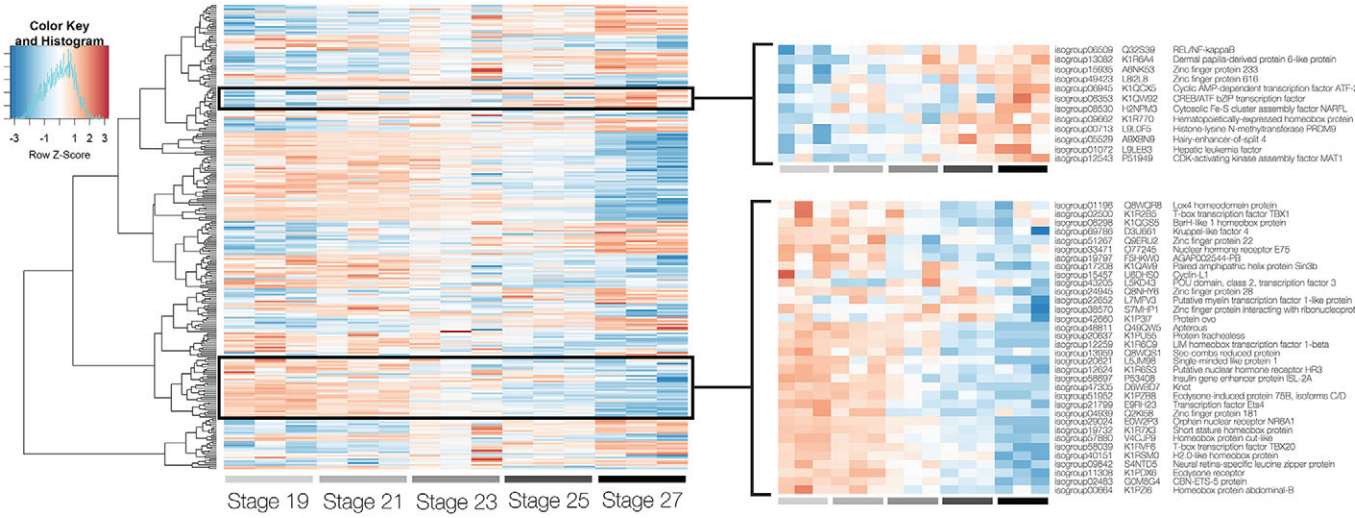

Fig. 9. Transcription factor-specific hierarchical clustering of time-course RNA-seq data from the eye and optic lobe. Statistically significant differentially expressed genes comparing stage 19 with stage 27 (FDR, 0.1).Top right panel shows a cluster of genes enriched later in development. Bottom right panel shows a cluster of genes enriched early in development.

Development (2016) 143, 3168-3181 doi:10.1242/dev.134254

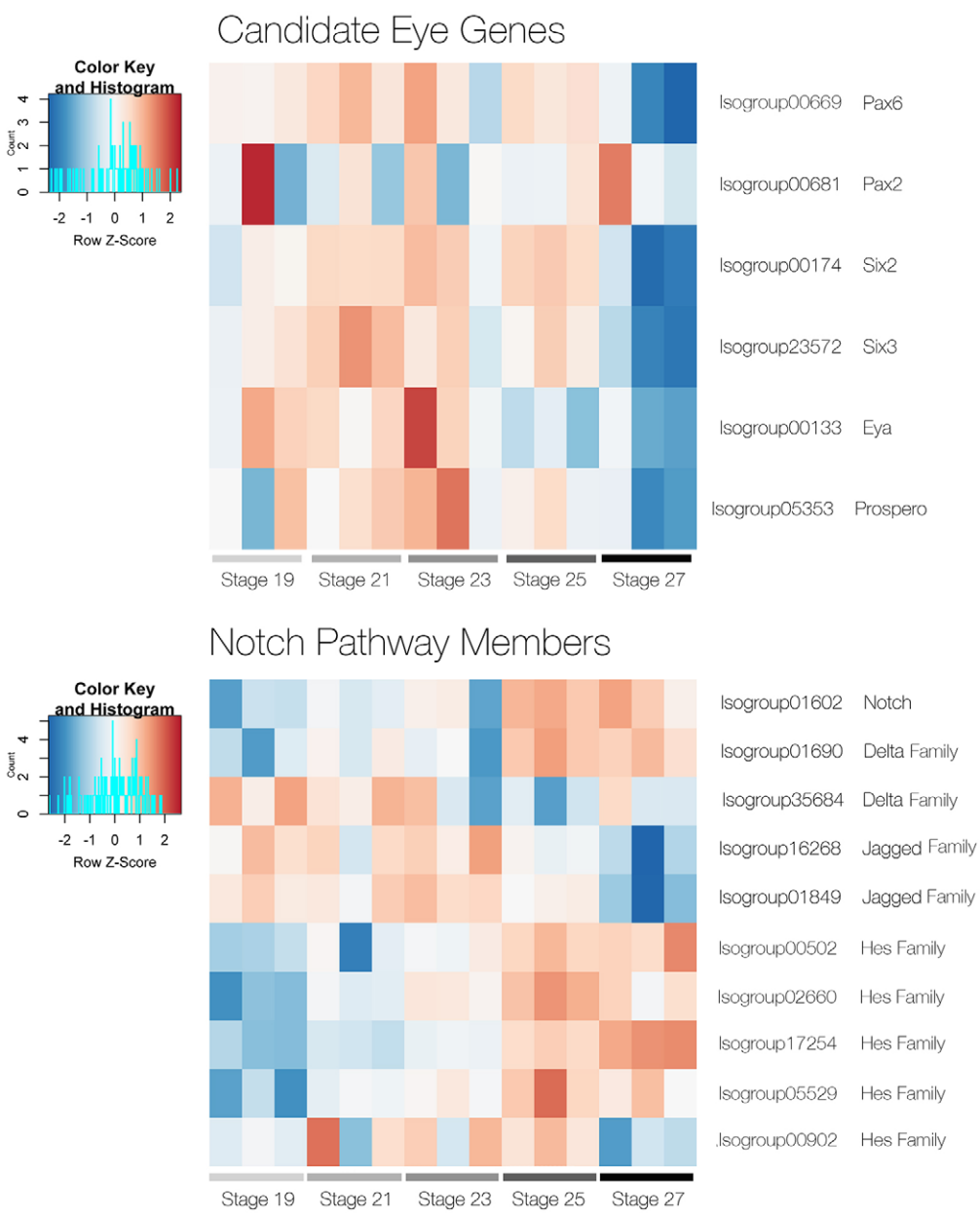

Fig. 10. Candidate gene RNA-seq heatmaps. Variance-stabilized transformed heatmaps for RDN genes, eye candidate genes and Notch pathway members. Genes identified by UniProt annotation and reciprocally Blasted against *Drosophila* and *Mus musculus* non-redundant protein database to confirm annotation. Multiple Delta, Jagged, and Hes family members were identified. Phylogenetic trees were constructed for all eye candidate genes, and Notch isogroup01602 and Hes isogroup00502 to confirm orthology (Fig. S3).

et al., 2013). Each of these systems has their strengths but the present models are relatively simple organisms. Cephalopods are a special group whose complex nervous system, unusual body plan and compelling behavior provide a unique opportunity to understand the evolution of complexity. Here, we establish a tractable system to study complex organ development and evolution. Our data generate an in-depth developmental resource to study a photoreceptive organ outside *Drosophila* and vertebrates and exciting opportunities now exist to probe the evolution of organogenesis and its genetic and cellular underpinnings.

Redrawing the cephalopod neural primordia map

We generated the first detailed fate map in any cephalopod species, and this empowers the field to draw new conclusions from old data. By generating these data, not only have we confirmed that the retina in *D. pealeii* arises from the eye placode and that the lens, cornea and iris are derived from the placode lip, but by combining them with gene expression studies, we also identified candidate genes likely to be involved in mediating cell fate specification events in these tissues (Arnold, 1965; Marthy, 1973; Naef, 1928). Furthermore, we do not detect cells incorporating into the eye from any other region, indicating that all eye tissue is derived solely from the placode and placode lip.

Previous studies utilized histology to identify ganglionic anlagen in the developing cephalopod nervous system (Yamamoto et al., 2003). Our fate map confirms and expands the region of cells contributing to the cerebral ganglia, as well as the region of cells contributing to the pedal ganglia. This supports recent findings in octopus and *Sepia officinalis* that suggest a broader neurogenic field and the cordal hypothesis (Shigeno et al., 2015; Buresi, 2016). Interestingly, our fate map identifies optic lobe progenitor cells in a drastically different location than formerly proposed (Naef, 1928; Yamamoto et al., 2003). Our data demonstrate that optic lobe progenitors lie dorsal to the placode, whereas previously, optic lobe primordia had been placed ventral to the placode. This displaces the previously identified palliovisceral primordia, suggesting that the

Development (2016) 143, 3168-3181 doi:10.1242/dev.134254

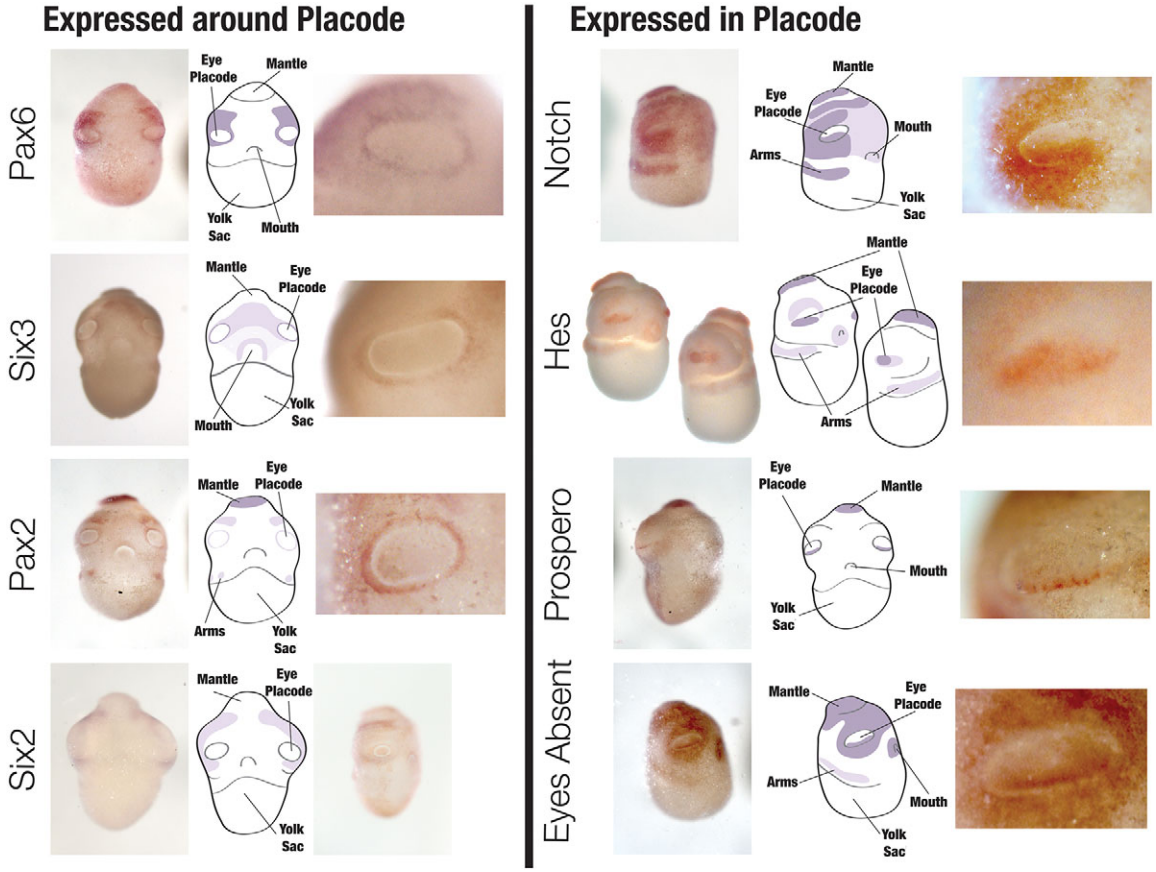

Fig. 11. Expression analysis of candidate eye genes at placode stages. *In situ* hybridization in early stage embryos. Cartoon depictions of the expression patterns next to the whole-embryo images. Higher magnification images shown of eye placode for all *in situ* results except *Six2*, where a lateral image of a stage 20 embryo is shown. *Six2* expression is restricted from the eye at stage 20. *Pax6*, *Six3*, *Pax2* and *Six2* are expressed in tissue surrounding the placode at stage 18 and excluded from the placode proper. *Notch*, *Hes*, *Prospero* and *Eya* are all expressed in the placode at stage 18. *Hes* expression is shown for both stages 18 (left) and 19 (right). *Hes* expression changes quickly from the ventral half of the placode at stage 18 to the entire placode at stage 19. The high-magnification image is for stage 18.

location of these progenitors is dorsal to the optic lobe progenitors. The redrawing of the neural primordial map enables the accurate interpretation of gene expression profiles from placode stage embryos onto later fates and dictate a reinterpretation of previous gene expression studies in other cephalopod species.

Correlating gene expression studies with cell fates

Capitalizing on the fate map, we superimpose gene expression patterns on this map and correlate gene products with late-stage ocular fates. *Pax6*, *Pax2*, and *Six3* are all co-expressed in the lip of the placode, and this region gives rise to the lens, cornea and iris (Fig. 12). The lens, cornea and iris are lineage-specific novelties in cephalopods, but interestingly, Pax6 and Six3 are required for lens induction in vertebrates (Ogino et al., 2012; Cvekl and Ashery-Padan, 2014). Currently, little is known about any lens-specific function of *eyeless* and *twin of eyeless* (Pax6 orthologs) in *Drosophila*, but imaginal disc cells expressing *eyeless* and *twin of eyeless* that give rise to the retina also

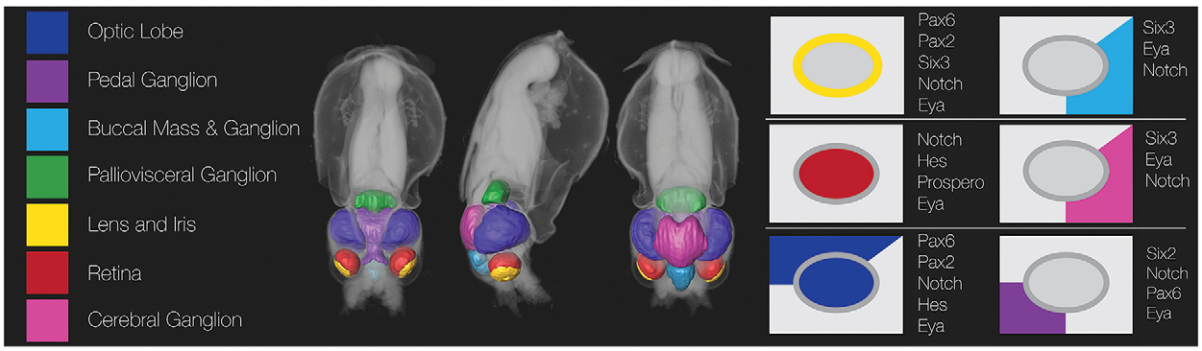

Fig. 12. Summary of DiI lineage tracing and gene expression analyses. The stage 18 fate map is color-coded with corresponding cell fates highlighted on the hatchling stage model. The model was generated from segmented reconstructions of microCT scan data. Placode stage gene expression profiles are correlated with the regions giving rise to distinct eye and brain regions.

Development (2016) 143, 3168-3181 doi:10.1242/dev.134254

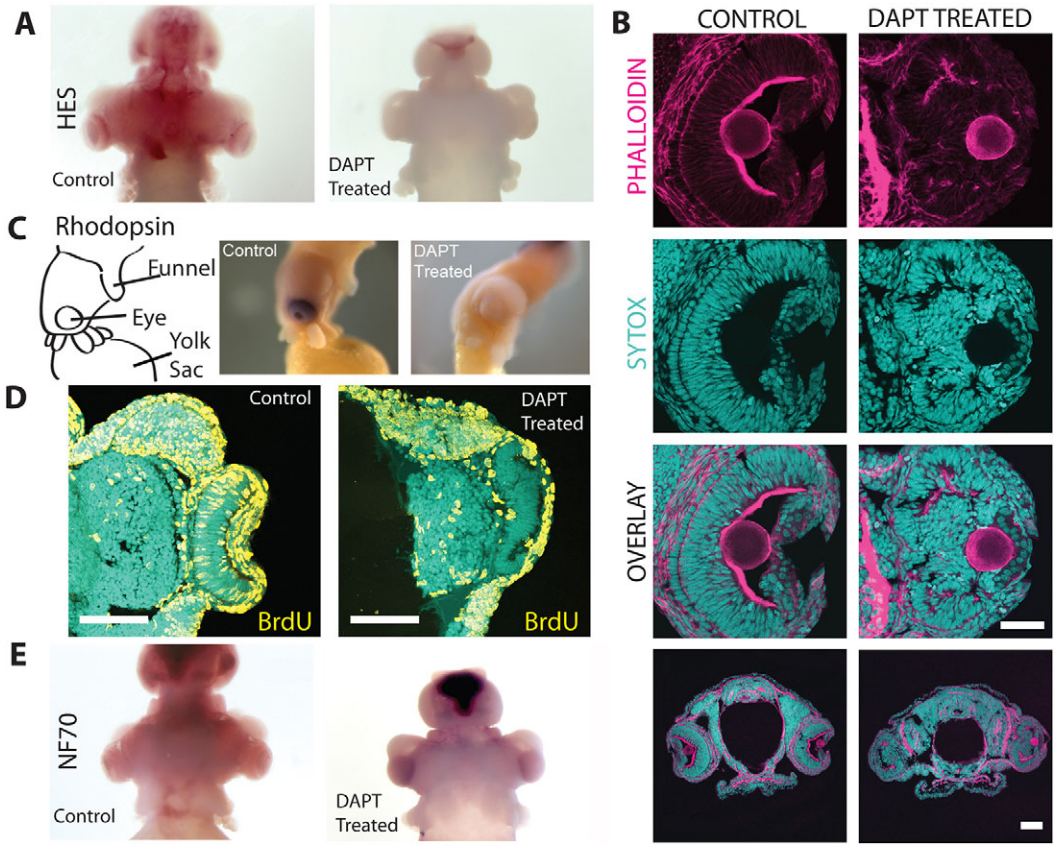

Fig. 13. Notch activity is required to maintain progenitor proliferation in the squid retina. (A) *Hes* expression is lost as a result of DAPT exposure (40 µM). *In situ* hybridization at stage 27 for *Hes* in DMSO and DAPT-treated embryos (anterior view). Mantle staining is a common background in cephalopods. (B) DAPT-treated embryos (20 µM) show disorganization and defects in photoreceptor differentiation. Scale bar: 50 µm for high magnification and 100 µm for low magnification. (C) DAPT (20 µM)-treated retinas lack *rhodopsin* expression suggesting a loss of differentiated photoreceptors. Lateral view of DMSO- and DAPT-treated embryos at stage 27. (D) DAPT (20 µM)-treated embryos express the neural marker *NF70*. Anterior view of embryos at stage 27. Scale bar: 50 µm. (E) DAPT (20 µM)-treated retinas fail to incorporate BrdU. Cross-sections of embryos. Embryos treated at stage 21 for 24 h, exposed to BrdU for 3 h and fixed immediately.

generate the lens (Charlton-Perkins et al., 2011a). *dPax2* is required for lens development in *Drosophila* but Pax2 does not play a known role in vertebrate lens formation (Fu and Noll, 1997). Pax2/5/8 was not found expressed in or around the eye and optic lobe in *Idiosepius notoides* until late stages, but is correlated with sensory systems in molluscs (Wollesen et al., 2015). Pax6 is broadly expressed in neurogenic tissues in other cephalopods, primarily optic lobe and eye regions, but also potentially in pedal ganglionic regions (Buresi, 2016).

There are three interpretations of the shared deployment of Pax and Six genes during lens formation. The first is that the tissue that generates the lens and the developmental origin of this tissue in *Drosophila*, vertebrates and cephalopods is homologous. This possibility supposes that in the common ancestor this tissue expressed Pax and Six genes and elaborated into the lens. In cephalopods and in *Drosophila*, the lens is derived from the same cells as, or adjacent cells to, the retina and therefore this tissue homology is plausible. However, in vertebrates, the lens placode is derived from the surface ectoderm and therefore is unlikely to be homologous. The second possibility is the concept of the cell as a unit of homology. This would suggest that a lens cell program existed in the common ancestor and this program included Pax and Six genes and was redeployed in the vertebrate surface ectoderm. This possibility is unlikely because crystallin proteins have evolved separately in each lineage, and there are many examples of photoreceptive organs found across the Bilateria lacking lenses (Jonasova and Kozmik, 2008; Oakley and Speiser, 2015 preprint). Moreover, lens tissue drastically differs across taxa, varying from cellular to acellular (Jonasova and Kozmik, 2008). These three lines of evidence suggest that no such lens cell existed in the common ancestor. Finally, the most plausible possibility is that Pax and Six gene involvement is homoplastic and independently evolved in lens formation. Pax transcription factor binding sites have been found upstream of crystallin genes, not only in vertebrates and *Drosophila*, but also in scallops and cnidarians (Piatigorsky, 2007). Pax involvement in lens formation in the cephalopod is one of many examples of this convergence. Currently, not enough is understood about the evolution of regulatory pathways to explain convergent gene regulation in independently evolved tissues. Ultimately, the results of this study highlight the need for better characterization of gene regulatory networks across the Bilateria to address questions regarding how networks elaborate and result in morphological complexity and diversity.

Beyond the placode lip, *Pax6* and *Pax2* are expressed in regions contributing to the squid optic lobe. *Pax6* also extends into the region contributing to the pedal ganglia. *Six3* is specifically expressed in the region contributing to the cerebral ganglia and *Six2* may play a role in pedal ganglia development. Interestingly, *Eya* has broad expression surrounding the retina, traversing all regions around the placode as well as the placode proper. It is possible that *Eya* also contributes to lens and iris development. This

Development (2016) 143, 3168-3181 doi:10.1242/dev.134254

is suggested by *Eya* expression in the cells surrounding the site of vesicle fusion and lens formation at stage 21 (Fig. S2G).

In squid, *Prospero* is expressed in a subset of cells on the ventral side of the retina placode. In *Drosophila*, *pros* specifies cone cells that generate the lens (Charlton-Perkins et al., 2011b). *Prox1*, the vertebrate homolog of *pros*, is involved in specification and differentiation of neurons within the retina as well as lens development (Wigle et al., 1999). In squid, *Prospero* does not appear to be expressed in the early lens-generating cells, but rather in the retina proper. This expression expands from a few cells to the entire retina later in development (Fig. S2C). This specific punctate expression at stage 18 suggests cell heterogeneity in the early retina primordia.

Notch signaling is a common mechanism regulating neuroepithelial differentiation across the Bilateria

It has been shown that Notch regulates differentiation in multiple bilaterian species and that non-canonical Notch regulates neural differentiation in cnidarians and may be ancestral to neural cell differentiation in the Bilateria (Louvi and Artavanis-Tsakonas, 2006; Layden and Martindale, 2014). The regulation of photoreceptor cell differentiation in the *Drosophila* eye was one of the first examples of Notch signaling functioning through lateral inhibition and this was subsequently demonstrated in the vertebrate retina, where Notch signaling is essential for vertebrate neurogenesis (Cagan and Ready, 1989; Austin et al., 1995; Pan and Rubin, 1997; Henrique et al., 1997; reviewed by Kumar, 2001; Louvi and Artavanis-Tsakonas, 2006). Work in zebrafish demonstrated that the Notch pathway influences neuronal differentiation in neuroepithelial cells undergoing interkinetic nuclear migration (IKNM). In the retina, a Notch gradient exposes the migrating progenitor cell nucleus to differing amounts of intracellular Notch depending on the phase of the cell cycle (Del Bene, 2008). In both the *Drosophila* eye disc, as well as in an elongated pseudostratified epithelium, loss of Notch signaling results in the premature differentiation of neural cell types and the loss of progenitor populations (Del Bene, 2008; Cagan and Ready, 1989).

Notch and Notch pathway members have been shown to function in annelid segmentation and to be expressed in the developing nervous system in *Capitella*. Our work is the first evaluation of Notch signaling in the lophotrochozoan photoreceptive organ that specifically addresses neurodifferentiation (Thamm and Seaver, 2008; Rivera, 2009). Our description of eye morphogenesis shows that the cephalopod retina is composed of a pseudostratified epithelial tissue, like the vertebrate retina, and that loss of Notch activity results in cell cycle exit and premature differentiation. IKNM has been identified as a shared aspect of pseudostratified epithelia and has been observed in multiple tissues in vertebrates, in the *Drosophila* wing disc and in *Nematostella*; however, this is the first description of IKNM in any lophotrochozoan (Meyer et al., 2011). Nuclear migration has been described in the *Drosophila* eye disc but not directly related to the process occurring in vertebrate neuroepithelial tissue, and it is not linked to the cell cycle (Tomlinson and Ready, 1987). Neurogenesis described in the lophotrochozoan *Capitella* sp. 1 shows the formation of a stratified epithelium through ingression of single epithelial cells from the anterior ectoderm (Meyer and Seaver, 2009). A similar mechanism has been predicted during neurogenesis of other brain regions in the cephalopod (Marthy, 1987). Our results in the retina support a mechanism governing differentiation and progenitor cell maintenance of photoreceptive neuroepithelial tissue regulated by Notch that may be shared by vertebrates and cephalopods. An in-depth understanding of IKNM and neuroepithelial formation more broadly in the Lophotrochozoa is necessary to better understand the cellular toolkit shared by the Bilateria to generate neural complexity.

Conclusions

Our goal is to establish the cephalopod eye as an accessible system to address questions regarding the evolution of nervous system complexity and gain insight into the nature of photoreception in the Urbilaterian ancestor. We have shown the potential of this system by identifying a case of convergence in the genetic network underlying formation of the cephalopod lens. These findings suggest a greater prevalence of homoplasy in the shared genetic networks underlying complex organs and highlight the significant amount of work that remains to better understand the nature of gene regulatory evolution.

Finally, this study also highlights cellular behaviors and characteristics that are likely to be fundamental to the development of nervous systems across the Bilateria. Building our understanding of the character of tissues and cells that are shared across species gives us greater insight into how complexity is built. Notch signaling enables the generation of multiple neural cell types. The organization of neuroepithelia and the process of IKNM may be the mechanism to achieve this complexity. It will be necessary to explore gene and protein expression of the Notch pathway in greater detail in the cephalopod as well as in other taxa, to understand how these mechanisms contribute to this process in the Urbilaterian ancestor. In all, this work opens a new avenue of investigation regarding the evolution of complexity and the emergence of novelty.

MATERIALS AND METHODS

Animal husbandry

Squid were acquired at the Marine Biological Laboratory, Woods Hole, MA. Embryos were cultured at 20°C.

Whole-embryo transcriptome and RNA-seq library preparation

Two embryos from the same egg sac of each stage, from 16-27, were prepared in TRIzol, phase separated and transferred to a Qiagen RNeasy column. Libraries were prepared after Meyer et al. (2009, 2012). Libraries were combined at equal volume and sequenced using 454 technology at the University of Texas, Austin. Eye and optic lobes tissues were dissected and prepared in TRIzol for RNA-seq. Libraries were prepared at the Vanderbilt VANTAGE laboratory using poly(A) selection and TruSeq library production and sequenced on an Illumina platform.

Assembly, annotation, mapping and statistical analysis

The 454 raw reads were processed using custom Perl scripts (Meyer and Seaver, 2009). Trimmed reads were assembled using Newbler v.2.6. Annotation was performed using BLASTX and custom Perl scripts mapped against the UniProt database (release 2014_09). Illumina data were processed for quality using custom Perl scripts (https://github.com/Eli-Meyer/sequence_processing). Reads were mapped to the reference transcriptome (Meyer et al., 2012). Raw read and assembly statistics are presented in Fig. S5. All raw reads and annotated data have been deposited at the NCBI (SRA accession numbers SRP065414 and SRP066528).

Time course clustering and differential gene expression analysis

Differential gene expression analysis and clustering was performed using the DESeq2 Bioconductor package v.1.10.1 run in R for Mac release 3.2.0 (Love et al., 2014). Data were exposed to log transformation and variance stabilizing transformation, analyzed for principal component analysis, variance and differential gene expression across stages. Analyses were performed on the whole dataset and subsets of the data, focusing on transcription factors (GO:0006355 and GO:0003700). The likelihood ratio test was performed by comparing stage 19 with stage 27. A false discovery rate of 0.1 was used to assess differential gene expression and the

Development (2016) 143, 3168-3181 doi:10.1242/dev.134254

hierarchical clustered heatmaps were generated based on Pearson correlation using heatmap.2 in the gplots package for R.

Alignment and trees

Sequence analysis was performed using Geneious (Kearse et al., 2012). Candidate sequences were identified through reciprocal Blast using *Drosophila* orthologs as bait. Isotig sequences were translated and trimmed for the ORF. Shared protein domains were identified using the PFAM database, identifying hidden Markov models (HMM) to search the rp-15 proteome database through the HMMER server (Bateman et al., 2004; Finn et al., 2011). A representative taxonomic subset of sequences and lophotrochozoan sequences were included in the final analysis. For Eya, no PFAM HMM is available. A sampling of the related proteins was generated with Blast using *Drosophila* Eya as bait. Multiple sequence alignment on the amino acid sequences were performed using the E-INS-I strategy in MAFFT (Katoh and Standley, 2013). We estimated support for a consensus tree from 1000 bootstrapped maximum likelihood trees for each phylogeny using PHYML (Guindon et al., 2010). Trees are shown unrooted (Fig. S3). Sequences are available in Table S2.

Cloning and *in situ* probe synthesis

RNA from a range of embryonic stages was reverse transcribed to create a cDNA library. Cloning primers are availabile in Table S1. cDNA sequences were verified by Sanger sequencing. Sense and antisense riboprobes were synthesized with digoxygenin-labeled rNTPs (Roche).

In situ hybridization

Embryos were fixed overnight in 4% paraformaldehyde and filtered seawater (FS). Embryos were transitioned into hybridization buffer (Hyb) (50% formamide, 5× SSC, 40 µl heparin, 0.25% Tween-20, 1% SDS, 200 mg yeast t-RNA). Embryos were incubated in Hyb at 65°C overnight. Probe was heated to 85°C in Hyb and applied to embryos overnight. Embryos were washed 3× in Hyb for 10 min and 2× for 60 min. Embryos were transitioned into 50% washes of 2× SSC for 20 min and 2× washes of 3× SSC for 20 min. Embryos were washed 2× in 0.2× SSC at room temperature for 5 min and 3× in PBS and 0.1% Triton X-100 (PT) for 5 min. Embryos were incubated in 5% normal goat serum and PT for 30 min and then incubated in alkaline-phosphatase-labeled anti-digoxygenin Fab fragments (Roche) at 1:2000 in PT-NGS overnight at 4°C. Embryos were washed with PT and reacted in BCIP/NBT solution.

Staging series

Embryos were fixed in 4% paraformaldehyde in FS overnight. Embryos were washed in PT and incubated in 25% sucrose for 60 min and 35% sucrose overnight. Embryos were embedded in Tissue Freezing Medium and 12 µm sections were cut. Three individuals were documented at each stage. Sections were stained with Sytox Green (5 µM) and Phalloidin (2.2 µM). Sections were mounted in Vectashield (Vector Labs) and visualized using confocal microscopy (Leica TCS SP5 II and Zeiss LSM-780 Quasar). Images are single *z*-planes.

BrdU incorporation assays

Embryos were exposed to 10 mM BrdU in FS with 100 units/ml penicillin and 100 µg/ml streptomycin (Pen-Strep FS) for 3 h and fixed immediately after exposure. Embryos were prepared and sectioned as above. Once sectioned, slides were rehydrated in PBS and incubated in 4 M HCl for 10 min at 37°C. Sections were washed in PBS and blocked with 5% NGS. Sections were incubated in rat anti-BrdU (Abcam, ab6326, 1:250) overnight at 4°C. Sections were washed in PBS and incubated in secondary antibody (Jackson ImmunoResearch, 112-175-143) for 2 h at room temperature. Embryos were washed in PBS for 2 h and exposed to Sytox Green as described above. Specimens were mounted in Vectashield (Vector Labs) and imaged using confocal microscopy.

TUNEL assays

TUNEL was performed according to the manufacturer's instructions (*In Situ* Cell Death Detection Kit; Roche, 12156792910). At least three individuals were examined for each stage.

Histology series

Embryos were fixed in 4% glutaraldehyde and 2% formaldehyde in seawater then incubated in a solution of 4% glutaraldehyde, 2% paraformaldehyde, 0.1 M sodium cacodylate, 2 mM Ca^{2+}, 4 mM Mg^{2+} overnight and washed with 0.1 M sodium cacodylate buffer. Embryos were incubated in 2% osmium tetroxide/4% potassium ferrocyanide/0.2 M sodium cacodylate buffer mix and microwaved under vacuum. The microwave was set to 100 W. Embryos were washed with deionized water, dehydrated with ethanol, transferred to an acetone solution, infiltrated with epoxy resin and baked for 2 days at 37°C. Embryos were sectioned at 0.7 µm, stained with Toluidine Blue and imaged using a Leica DM2500 microscope. At least three individuals were examined for each stage.

MicroCT

Hatchlings were fixed in 4% glutaraldehyde and 2% paraformaldehyde in FS. Hatchlings were washed in PBS and stained with 0.1% iodine/0.2% potassium iodide in water. Specimens were dehydrated overnight into ethanol and scanned using the Xradia microCT Scanner at the University of Texas high-resolution CT facility.

Lineage tracing

A stock solution of 5 µg/µl of CellTracker CM-DiI (Invitrogen) in ethanol was diluted into vegetable oil (0.5 µg/µl). Embryos were reared in 12-well culture dishes on 1% agarose in Pen-Strep FS and then fixed in 4% paraformaldehyde. Specimens were imaged then embedded, cryosectioned and re-imaged.

DAPT treatments

Embryos were dissected from chorions and incubated in 20 µM or 40 µM DAPT dissolved in 1% DMSO and Pen-Strep FS. Embryos were cultured in groups of seven or less. Experiments included over 20 embryos per exposure. Control embryos were incubated in 1% DMSO in Pen-Strep FS. Embryos were exposed for 24 h and either fixed immediately, exposed to BrdU for 3 h and fixed or allowed to recover and grow to stage 27 and fixed. At least three individuals were examined for each experiment.

Acknowledgements

The authors acknowledge the Texas Advanced Computing Center (TACC) at The University of Texas at Austin for providing HPC, visualization, database or grid resources that have contributed to the research results reported within this paper. URL: http://www.tacc.utexas.edu. MicroCT data were obtained at the High-Resolution X-ray Computed Tomography Facility of the University of Texas at Austin. We are grateful to Joe Digiorgis, Josh Rosenthal, Andrew Gillis and members of the Gross lab for critical discussion and suggestions on this work, to Dwight Romanowicz for assistance with histology, to Jerry Dammers and Jennifer Moore for assistance with image processing, and to the staff of the Marine Resource Center at the Marine Biological Laboratory in Woods Hole for assistance with embryo collection.

Competing interests

The authors declare no competing or financial interests.

Author contributions

Conceived of project: K.M.K., J.M.G. Designed experiments: K.M.K., J.M.G. Executed experiments: K.M.K., P.S. Analyzed data: K.M.K., J.M.G., E.M. Wrote manuscript: K.M.K. Edited manuscript: K.M.K., J.M.G.

Funding

This work was funded by a fellowship from the Grass Foundation to K.M.K.; a Plum Foundation Research Award; a H. Keffer Hartline and Edward MacNichol, Jr. Fellowship Award; a Laura and Arthur Colwin Endowed Summer Research Fellowship Fund Award; and a National Science Foundation CAREER Award [IOS-0745782 to J.M.G.].

Data availability

All raw reads and annotated data have been deposited at the NCBI (http://www.ncbi.nlm.nih.gov/sra; SRA accession numbers SRP065414 and SRP066528).

Supplementary information

Supplementary information available online at
http://dev.biologists.org/lookup/doi/10.1242/dev.134254.supplemental

Development (2016) 143, 3168-3181 doi:10.1242/dev.134254

References

Albertin, C. B., Simakov, O., Mitros, T., Wang, Z. Y., Pungor, J. R., Edsinger-Gonzales, E., Brenner, S., Ragsdale, C. W. and Rokhsar, D. S. (2015). The octopus genome and the evolution of cephalopod neural and morphological novelties. *Nature* **524**, 220-224.

Allen, R. D., Metuzals, J., Tasaki, I., Brady, S. T. and Gilbert, S. P. (1982). Fast axonal transport in squid giant axon. *Science* **218**, 1127-1129.

Alon, S., Garrett, S. C., Levanon, E. Y., Olson, S., Graveley, B. R., Rosenthal, J. J. C. and Eisenberg, E. (2015). The majority of transcripts in the squid nervous system are extensively recoded by A-to-I RNA editing. *Elife* **4**, e05198.

Arendt, D. (2003). Evolution of eyes and photoreceptor cells types. *Int. J. Dev. Biol.* **47**, 563-571.

Arnold, J. M. (1965). Normal embryonic stages of the squid, *Loligo pealii* (Lesueur). *Biol. Bull.* **128**, 24-32.

Arnold, J. M. (1966). On the occurrence of microtubules in the developing lens of the squid Loligo pealii. *J. Ultrastruct. Res.* **14**, 534-539.

Arnold, J. M. (1967). Fine structure of the development of the cephalopod lens. *J. Ultrastruct. Res.* **17**, 527-543.

Arnold, J. M. and Williams-Arnold, L. D. (1976). The egg cortex problem as seen through the squid eye. *Am. Zool.* **16**, 421-446.

Austin, C. P., Feldman, D. E., Ida, J. A. and Cepko, C. L. (1995). Vertebrate retinal ganglion cells are selected from competent progenitors by the action of Notch. *Development* **121**, 3637-3650.

Baker, N. E. (2001). Cell proliferation, survival, and death in the Drosophila eye. *Semin. Cell Dev. Biol.*, **12**, 499-507.

Baratte, S., Andouche, A. and Bonnaud, L. (2007). Engrailed in cephalopods: a key gene related to the emergence of morphological novelties. *Dev. Genes Evol.* **217**, 353-362.

Bassaglia, Y., Bekel, T., Da Silva, C., Poulain, J., Andouche, A., Navet, S. and Bonnaud, L. (2012). ESTs library from embryonic stages reveals tubulin and reflectin diversity in *Sepia officinalis* (Mollusca—Cephalopoda). *Gene* **498**, 203-211.

Bateman, A., Coin, L., Durbin, R., Finn, R. D., Hollich, V., Griffiths-Jones, S., Khanna, A., Marshall, M., Moxon, S., Sonnhammer, E. L. et al. (2004). The Pfam protein families database. *Nucleic Acids Res.* **32** Suppl. 1, D138-D141.

Baye, L. M. and Link, B. A. (2008). Nuclear migration during retinal development. *Brain Res.* **1192**, 29-36.

Blair, S. S. (1999). Eye development: Notch lends a handedness. *Curr. Biol.* **9**, R356-R360.

Brady, S. T., Lasek, R. J. and Allen, R. D. (1982). Fast axonal transport in extruded axoplasm from squid giant axon. *Science* **218** 1129-1131.

Buresi, A., Baratte, S., Da Silva, C. and Bonnaud, L. (2012). orthodenticle/otx ortholog expression in the anterior brain and eyes of *Sepia officinalis* (Mollusca, Cephalopoda). *Gene Expr. Patterns* **12**, 109-116.

Buresi, A., Canali, E., Bonnaud, L. and Baratte, S. (2013). Delayed and asynchronous ganglionic maturation during cephalopod neurogenesis as evidenced by Sof-elav1 expression in embryos of *Sepia officinalis* (Mollusca, Cephalopoda). *J. Comp. Neurol.* **521**, 1482-1496.

Buresi, A., Andouche, A., Navet, S., Bassaglia, Y., Bonnaud-Ponticelli, L. and Baratte, S. (2016). Nervous system development in cephalopods: How egg yolk-richness modifies the topology of the mediolateral patterning system. *Dev. Biol.* **415**, 143-156.

Cagan, R. L. and Ready, D. F. (1989). Notch is required for successive cell decisions in the developing Drosophila retina. *Genes Dev.* **3**, 1099-1112.

Charlton-Perkins, M., Brown, N. L. and Cook, T. A. (2011a). The lens in focus: a comparison of lens development in *Drosophila* and vertebrates. *Mol. Genet. Genomics* **286**, 189-213.

Charlton-Perkins, M., Whitaker, S. L., Fei, Y., Xie, B., Li-Kroeger, D., Gebelein, B. and Cook, T. (2011b). Prospero and Pax2 combinatorially control neural cell fate decisions by modulating Ras- and Notch-dependent signaling. *Neural Dev.* **6**, 20.

Cvekl, A. and Ashery-Padan, R. (2014). The cellular and molecular mechanisms of vertebrate lens development. *Development* **141**, 4432-4447.

Darwin, C. (1859). *On the Origin of Species*, p. 360. London: Murray.

Del Bene, F., Wehman, A. M., Link, B. A. and Baier, H. (2008). Regulation of neurogenesis by interkinetic nuclear migration through an apical-basal notch gradient. *Cell* **134**, 1055-1065.

Dorsky, R. I., Rapaport, D. H. and Harris, W. A. (1995). Xotch inhibits cell differentiation in the Xenopus retina. *Neuron* **14**, 487-496.

Farfán, C., Shigeno, S., Nödl, M.-T. and de Couet, H. G. (2009). Developmental expression of apterous/Lhx2/9 in the sepiolid squid Euprymna scolopes supports an ancestral role in neural development. *Evol. Dev.* **11**, 354-362.

Fernald, R. D. (2006). Casting a genetic light on the evolution of eyes. *Science* **313**, 1914-1918.

Ferrier, D. E. K. (2012). Evolutionary crossroads in developmental biology: annelids. *Development* **139**, 2643-2653.

Finn, R. D., Clements, J. and Eddy, S. R. (2011). HMMER web server: interactive sequence similarity searching. *Nucleic Acids Res.* **39**, W29-W37.

Focareta, L., Sesso, S. and Cole, A. G. (2014). Characterization of homeobox genes reveals sophisticated regionalization of the central nervous system in the European cuttlefish *Sepia officinalis*. *PLoS ONE* **9**, e109627.

Fu, W. and Noll, M. (1997). The Pax2 homolog sparkling is required for development of cone and pigment cells in the Drosophila eye. *Genes Dev.* **11**, 2066-2078.

Gehring, W. J. (1996). The master control gene for morphogenesis and evolution of the eye. *Genes Cells* **1**, 11-15.

Gehring, W. J. (2005). New perspectives on eye development and the evolution of eyes and photoreceptors. *J. Hered.* **96**, 171-184.

Gehring, W. J. and Ikeo, K. (1999). Pax 6: mastering eye morphogenesis and eye evolution. *Trends Genet.* **15**, 371-377.

Geling, A., Steiner, H., Willem, M., Bally-Cuif, L. and Haass, C. (2002). A γ-secretase inhibitor blocks Notch signaling in vivo and causes a severe neurogenic phenotype in zebrafish. *EMBO Rep.* **3**, 688-694.

Gentile, L., Cebrià, F. and Bartscherer, K. (2011). The planarian flatworm: an in vivo model for stem cell biology and nervous system regeneration. *Dis. Model. Mech.* **4**, 12-19.

Gilbert, D. L., Adelman, W. J., and Arnold, J. M. (1990). *Squid as Experimental Animals*. New York: Springer Science & Business Media.

Go, M. J., Eastman, D. S. and Artavanis-Tsakonas, S. (1998). Cell proliferation control by Notch signaling in Drosophila development. *Development* **125**, 2031-2040.

Guindon, S., Dufayard, J. F., Lefort, V., Anisimova, M., Hordijk, W. and Gascuel, O. (2010). New algorithms and methods to estimate maximum-likelihood phylogenies: assessing the performance of PhyML 3.0. *Syst. Biol.* **59**, 307-321.

Halder, G., Callaerts, P. and Gehring, W. J. (1995). New perspectives on eye evolution. *Curr. Opin. Genet. Dev.* **5**, 602-609.

Hartmann, B., Lee, P. N., Kang, Y. Y., Tomarev, S., De Couet, H. G. and Callaerts, P. (2003). Pax6 in the sepiolid squid Euprymna scolopes: evidence for a role in eye, sensory organ and brain development. *Mech. Dev.* **120**, 177-183.

Henrique, D., Hirsinger, E., Adam, J., Le Roux, I., Pourquié, O., Ish-Horowicz, D. and Lewis, J. (1997). Maintenance of neuroepithelial progenitor cells by Delta–Notch signalling in the embryonic chick retina. *Curr. Biol.* **7**, 661-670.

Henry, J. J., Collin, R. and Perry, K. J. (2010). The slipper snail, Crepidula: an emerging lophotrochozoan model system. *Biol. Bull.* **218**, 211-229.

Hobert, O. and Westphal, H. (2000). Functions of LIM-homeobox genes. *Trends Genet.* **16**, 75-83.

Hodgkin, A. L. and Huxley, A. F. (1952a). Currents carried by sodium and potassium ions through the membrane of the giant axon of *Loligo*. *J. Physiol.* **116**, 449-472.

Hodgkin, A. L. and Huxley, A. F. (1952b). The dual effect of membrane potential on sodium conductance in the giant axon of Loligo. *J. Physiol.* **116**, 497-506.

Hodgkin, A. L. and Katz, B. (1949). The effect of sodium ions on the electrical activity of the giant axon of the squid. *J. Physiol.* **108**, 37-77.

Hodgkin, A. L., Huxley, A. F. and Katz, B. (1952). Measurement of current-voltage relations in the membrane of the giant axon of *Loligo*. *J. Physiol.* **116**, 424.

Jonasova, K. and Kozmik, Z. (2008). Eye evolution: lens and cornea as an upgrade of animal visual system. *Semin. Cell Dev. Biol.* **19**, 71-81.

Katoh, K. and Standley, D. M. (2013). MAFFT multiple sequence alignment software version 7: improvements in performance and usability. *Mol. Biol. Evol.* **30**, 772-780.

Kearse, M., Moir, R., Wilson, A., Stones-Havas, S., Cheung, M., Sturrock, S., Buxton, S., Cooper, A., Markowitz, S., Duran, C. et al. (2012). Geneious Basic: an integrated and extendable desktop software platform for the organization and analysis of sequence data. *Bioinformatics* **28**, 1647-1649.

Kerbl, A., Handschuh, S., Nödl, M.-T., Metscher, B., Walzl, M. and Wanninger, A. (2013). Micro-CT in cephalopod research: investigating the internal anatomy of a sepiolid squid using a non-destructive technique with special focus on the ganglionic system. *J. Exp. Mar. Biol. Ecol.* **447**, 140-148.

Kumar, J. P. (2001). Signalling pathways in Drosophila and vertebrate retinal development. *Nat. Rev. Genet.* **2**, 846-857.

Kumar, J. P. (2010). 1 Retinal determination: the beginning of eye development. *Curr. Top. Dev. Biol.* **93**, 1-28.

Land, M. F. and Fernald, R. D. (1992). The evolution of eyes. *Annu. Rev. Neurosci.* **15**, 1-29.

Lapan, S. W. and Reddien, P. W. (2012). Transcriptome analysis of the planarian eye identifies ovo as a specific regulator of eye regeneration. *Cell Rep.* **2**, 294-307.

Layden, M. J. and Martindale, M. Q. (2014). Non-canonical Notch signaling represents an ancestral mechanism to regulate neural differentiation. *Evodevo* **5**, 30.

Lee, P. N., Callaerts, P., de Couet, H. G. and Martindale, M. Q. (2003). Cephalopod Hox genes and the origin of morphological novelties. *Nature* **424**, 1061-1065.

Livesey, F. J. and Cepko, C. L. (2001). Vertebrate neural cell-fate determination: lessons from the retina. *Nat. Rev. Neurosci.* **2**, 109-118.

Louvi, A. and Artavanis-Tsakonas, S. (2006). Notch signalling in vertebrate neural development. *Nat. Rev. Neurosci.* **7**, 93-102.

Love, M. I., Huber, W. and Anders, S. (2014). Moderated estimation of fold change and dispersion for RNA-seq data with DESeq2. *Genome Biol.* **15**, 550.

Marthy, H. J. (1973). An experimental study of eye development in the cephalopod Loligo vulgaris: determination and regulation during formation of the primary optic vesicle. *J. Embryol. Exp. Morphol.* **29**, 347-361.
Marthy, H. J. (1987). Ontogenesis of the nervous system in cephalopods. In *Nervous Systems in Invertebrates* (ed. M. A. Ali), pp. 443-459. US: Springer.
Mears, A. J., Kondo, M., Swain, P. K., Takada, Y., Bush, R. A., Saunders, T. L., Sieving, P. A. and Swaroop, A. (2001). Nrl is required for rod photoreceptor development. *Nat. Genet.* **29**, 447-452.
Meyer, N. P. and Seaver, E. C. (2009). Neurogenesis in an annelid: characterization of brain neural precursors in the polychaete Capitella sp. I. *Dev. Biol.* **335**, 237-252.
Meyer, E., Aglyamova, G. V., Wang, S., Buchanan-Carter, J., Abrego, D., Colbourne, J. K., Willis, B. L. and Matz, M. V. (2009). Sequencing and de novo analysis of a coral larval transcriptome using 454 GSFlx. *BMC Genomics* **10**, 219.
Meyer, E. J., Ikmi, A. and Gibson, M. C. (2011). Interkinetic nuclear migration is a broadly conserved feature of cell division in pseudostratified epithelia. *Curr. Biol.* **21**, 485-491.
Meyer, E., Logan, T. L. and Juenger, T. E. (2012). Transcriptome analysis and gene expression atlas for Panicum hallii var. filipes, a diploid model for biofuel research. *Plant J.* **70**, 879-890.
Naef, A. (1928). Die Cephalopoden (Embryologie). *Fauna Flora Golf Neapel* **35**, 1-357.
Navet, S., Andouche, A., Baratte, S. and Bonnaud, L. (2009). Shh and Pax6 have unconventional expression patterns in embryonic morphogenesis in Sepia officinalis (Cephalopoda). *Gene Expr. Patterns* **9**, 461-467.
Nepveu, A. (2001). Role of the multifunctional CDP/Cut/Cux homeodomain transcription factor in regulating differentiation, cell growth and development. *Gene* **270**, 1-15.
Nilsson, D.-E. (2004). Eye evolution: a question of genetic promiscuity. *Curr. Opin. Neurobiol.* **14**, 407-414.
Nilsson, D.-E. (2013). Eye evolution and its functional basis. *Visual Neurosci.* **30**, 5-20.
Nixon, M. and Young, J. Z. (2003). *The Brains and Lives of Cephalopods*. New York: Oxford University Press.
Oakley, T. H. and Speiser, D. I. (2015). How complexity originates: the evolution of animal eyes. *bioRxiv*. doi:10.1101/017129.
Ogino, H., Ochi, H., Reza, H. M. and Yasuda, K. (2012). Transcription factors involved in lens development from the preplacodal ectoderm. *Dev. Biol.* **363**, 333-347.
Ogura, A., Yoshida, M. A., Moritaki, T., Okuda, Y., Sese, J., Shimizu, K. K., Sousounis, K. and Tsonis, P. A. (2013). Loss of the six3/6 controlling pathways might have resulted in pinhole-eye evolution in Nautilus. *Sci. Rep.* **3**, 1432.
Pan, D. and Rubin, G. M. (1997). Kuzbanian controls proteolytic processing of Notch and mediates lateral inhibition during Drosophila and vertebrate neurogenesis. *Cell* **90**, 271-280.
Peyer, S. M., Pankey, M. S., Oakley, T. H. and McFall-Ngai, M. J. (2014). Eye-specification genes in the bacterial light organ of the bobtail squid *Euprymna scolopes*, and their expression in response to symbiont cues. *Mech. Dev.* **131**, 111-126.
Piatigorsky, J. (2007). *Gene Sharing and Evolution: The Diversity of Protein Functions*, p. 1. Cambridge, MA: Harvard University Press.
Reig, G., Cabrejos, M. E. and Concha, M. L. (2007). Functions of BarH transcription factors during embryonic development. *Dev. Biol.* **302**, 367-375.
Rosenfeld, M. G. (1991). POU-domain transcription factors: pou-er-ful developmental regulators. *Genes Dev.* **5**, 897-907.
Rivera, A. S. and Weisblat, D. A. (2009). And Lophotrochozoa makes three: Notch/Hes signaling in annelid segmentation. *Dev. Genes Evol.* **219**, 37-43.
Schnitzler, C. E., Pang, K., Powers, M. L., Reitzel, A. M., Ryan, J. F., Simmons, D., Tada, T., Park, M., Gupta, J., Brooks, S. Y. et al. (2012). Genomic organization, evolution, and expression of photoprotein and opsin genes in Mnemiopsis leidyi: a new view of ctenophore photocytes. *BMC Biol.* **10**, 107.
Shigeno, S., Parnaik, R., Albertin, C. B. and Ragsdale, C. W. (2015). Evidence for a cordal, not ganglionic, pattern of cephalopod brain neurogenesis. *Zool. Lett.* **1**, 1-13.
Simakov, O., Marletaz, F., Cho, S.-J., Edsinger-Gonzales, E., Havlak, P., Hellsten, U., Kuo, D.-H., Larsson, T., Lv, J., Arendt, D. et al. (2013). Insights into bilaterian evolution from three spiralian genomes. *Nature* **493**, 526-531.
Szaro, B. G., Pan, H. C., Wa, J. and Battey, J. (1991). Squid low molecular weight neurofilament proteins are a novel class of neurofilament protein. A nuclear lamin-like core and multiple distinct proteins formed by alternative RNA processing. *J. Biol. Chem.* **266**, 15035-15041.
Thamm, K. and Seaver, E. C. (2008). Notch signaling during larval and juvenile development in the polychaete annelid Capitella sp. I. *Dev. Biol.* **320**, 304-318.
Tomarev, S. I. (1997). Pax-6, Eyes absent, and Prox 1 in eye development. *Int. J. Dev. Biol* **41**, 835-842.
Tomarev, S. I., Callaerts, P., Kos, L., Zinovieva, R., Halder, G., Gehring, W. and Piatigorsky, J. (1997). Squid Pax-6 and eye development. *Proc. Natl. Acad. Sci. USA* **94** 2421-2426.
Tomita, K., Ishibashi, M., Nakahara, K., Ang, S.-L., Nakanishi, S., Guillemot, F. and Kageyama, R. (1996). Mammalian hairy and Enhancer of split homolog 1 regulates differentiation of retinal neurons and is essential for eye morphogenesis. *Neuron* **16**, 723-734.
Tomlinson, A. and Ready, D. F. (1987). Neuronal differentiation in the Drosophila ommatidium. *Dev. Biol.* **120**, 366-376.
Vale, R. D., Schnapp, B. J., Reese, T. S. and Sheetz, M. P. (1985a). Movement of organelles along filaments dissociated from the axoplasm of the squid giant axon. *Cell* **40**, 449-454.
Vale, R. D., Schnapp, B. J., Reese, T. S. and Sheetz, M. P. (1985b). Organelle, bead, and microtubule translocations promoted by soluble factors from the squid giant axon. *Cell* **40**, 559-569.
Vecino, E., Hernández, M. and García, M. (2004). Cell death in the developing vertebrate retina. *Int. J. Dev. Biol.* **48**, 965-974.
von Salvini-Plawen, L. and Mayr, E. (1977). On the evolution of photoreceptors and eyes. *Evol. Biol.* **10**, 207-263.
Wagner, G. P. (2014). *Homology, Genes, and Evolutionary Innovation*. Princeton: Princeton Univ Press.
West, J. A., Sivak, J. G., Pasternak, J. and Piatigorsky, J. (1994). Immunolocalization of S-crystallins in the developing squid (*Loligo opalescens*) lens. *Dev. Dyn.* **199**, 85-92.
West, J. A., Sivak, J. G. and Doughty, M. J. (1995). Microscopical evaluation of the crystalline lens of the squid (*Loligo opalescens*) during embryonic development. *Exp. Eye Res.* **60**, 19-35.
Wigle, J. T., Chowdhury, K., Gruss, P. and Oliver, G. (1999). Prox1 function is crucial for mouse lens-fibre elongation. *Nat. Genet.* **21**, 318-322.
Wild, E., Wollesen, T., Haszprunar, G. and Heß, M. (2015). Comparative 3D microanatomy and histology of the eyes and central nervous systems in coleoid cephalopod hatchlings. *Organism. Divers. Evol.* **15**, 37-64.
Wollesen, T., McDougall, C., Degnan, B. M. and Wanninger, A. (2014). POU genes are expressed during the formation of individual ganglia of the cephalopod central nervous system. *EvoDevo* **5**, 41.
Wollesen, T., Monje, S. V. R., Todt, C., Degnan, B. M. and Wanninger, A. (2015). Ancestral role of Pax2/5/8 in molluscan brain and multimodal sensory system development. *BMC Evol. Biol.* **15**, 231.
Yamamoto, M. (1985). Ontogeny of the visual system in the cuttlefish, Sepiella japonica. I. Morphological differentiation of the visual cell. *J. Comp. Neurol.* **232**, 347-361.
Yamamoto, M., Takasu, N. and Uragami, I. (1985). Ontogeny of the visual system in the cuttlefish, *Sepiella japonica*. II. Intramembrane particles, histofluorescence, and electrical responses in the developing retina. *J. Comp. Neurol.* **232**, 362-371.
Yamamoto, M., Shimazaki, Y. and Shigeno, S. (2003). Atlas of the embryonic brain in the pygmy squid, Idiosepius paradoxus. *Zool. Sci.* **20**, 163-179.
Yoshida, M. A. and Ogura, A. (2011). Genetic mechanisms involved in the evolution of the cephalopod camera eye revealed by transcriptomic and developmental studies. *BMC Evol. Biol.* **11**, 180.
Yoshida, M. A., Yura, K. and Ogura, A. (2014). Cephalopod eye evolution was modulated by the acquisition of Pax-6 splicing variants. *Sci. Rep.* **4**, 4256.
Young, J. Z. (1962a). The retina of cephalopods and its degeneration after optic nerve section. *Philos. Trans. R. Soc. B Biol. Sci.* **245**, 1-18.
Young, J. Z. (1962b). The optic lobes of Octopus vulgaris. *Philos. Trans. R. Soc. B Biol. Sci.* **245**, 19-58.
Young, J. Z. (1971). *Anatomy of the Nervous System of Octopus vulgaris*. Oxford, UK: Oxford University Press.
Zantke, J., Bannister, S., Rajan, V. B. V., Raible, F. and Tessmar-Raible, K. (2014). Genetic and genomic tools for the marine annelid Platynereis dumerilii. *Genetics* **197**, 19-31.
Zonana, H. V. (1961). Fine Structure of the squid retina. *Bull. Johns Hopkins Hospital* **109**, 185-205.